High resolution interferometry as a tool for characterization of swelling of weakly charged hydrogels subjected to amphiphile and cyclodextrin exposure

.

Ming Gao, Kamila Gawel, and Bjørn Torger Stokke*

Biophysics and Medical Technology, Department of Physics

The Norwegian University of Science and Technology, NTNU

NO-7491 Trondheim, NORWAY

* To whom correspondence should be addressed: Phone: +47 73 59 34 34; Fax: +47 73 59 77 10; E-mail: bjorn.stokke@ntnu.no

Abstract

A high resolution interferometric technique was used to determine swelling behavior of weakly charged polyacrylamide hydrogels in the presence of oppositely charged surfactants and subsequent exposure to cyclodextrins. Hydrogels of copolymerized acrylamide and 2-acrylamido-2-methyl-1-propanesulfonic acid (0.22, 0.44, 0.88 mol%) and crosslinked with bisacrylamide (3, 6, 12 mol%) were employed. The equilibrium swelling and swelling kinetics of the hydrogels were determined with 2 nanometer resolution of the optical length and sampled at approximately 1 Hz. These properties were determined for the hydrogels exposed to cationic surfactants dodecyltrimethylammonium bromide (DTAB) and cetyltrimethylammonium bromide (CTAB) at concentrations from 10^{-7} up to $2 \cdot 10^{-3}$ M. The distribution of surfactants within AAM-co-AMPSA hydrogel was investigated by confocal laser scanning microscopy imaging of chosen hydrogel equilibrated in CTAB/perylene solution. Hydrogels equilibrated at selected surfactant concentrations were subsequently exposed to cyclodextrins (α-CD, β-CD, methyl-β-CD and γ-CD) forming inclusion complexes with the surfactants. The results show different type of behavior for the two surfactants used, arising from the differences in the length of surfactant hydrophobic tail. The changes in the surfactant induced swelling of the hydrogels are suggested to arise from the net effect of electrostatic screening of sulfonic acid – amide group interactions and surfactant micellization. Hydrogels with the largest charge density and lowest crosslink density yielded the most pronounced changes in swelling properties on exposure to DTAB or CTAB. The hydrogels displayed swelling kinetics on stepwise changes in surfactant concentrations that depended on the surfactant concentration range. The high resolution monitoring of hydrogel swelling associated with supramolecular complex formation in a three-component system hydrogel - amphiphilic molecule - cyclodextrin provide more details in the swelling behavior than previously disclosed.

Keywords: Hydrogel; Interferometry; Nanometer resolution; Cationic surfactant; Cyclodextrin; Inclusion complex;

1. Introduction

Fiber optic-based interferometry is a well suited technique for high resolution determination of hydrogel volume changes [1]. It has already proved its potential in sensing such analytes as glucose [2, 3] and oligonucleotides [4-6]. Herein we present the technique as a useful tool for label-free monitoring of swelling phenomena occurring in various hydrogel-amphiphile and hydrogel- amphiphile-macrocycle cases.

Hydrogels, capable to swell and retain large volumes of water in their swollen structure, are known to form stable complexes with amphiphilic molecules such proteins/peptides [7, 8], lipids [9, 10], and surfactants [11-15]. Hydrogel-amphiphile systems have been developed and characterized due to potential applications within controlled drug release [16-18], pollutants removal [19-21], enhanced oil recovery [22], or microheterogeneous catalysis [23, 24]. Ionic hydrogels shows adsorption properties towards oppositely charged amphiphiles. Association of charged surfactants inside hydrogel is driven by coupled hydrophobic and electrostatic effects [25]. Release of counterions associated with the charged polymeric chains contributes through an entropic mechanism to the association [25]. Surfactants interacting with oppositely charged linear or crosslinked polymers tend to aggregate at concentrations much lower than their critical micelle concentration (cmc) in solution [26-28]. The presence of interacting polyelectrolytes decreases the repulsive interactions between the surfactant molecules resulting in micelles being formed at a critical aggregation concentration (cac) lower than the cmc. Such surfactant aggregation within hydrogel networks induces volume transitions [15, 25, 29]. The critical collapse concentration (ccc), referring to the surfactant concentration at the onset of the hydrogel transition, is reported to nearly coincide with the cac [25]. While swelling behavior of highly charged hydrogels upon exposure to oppositely charged surfactants already has been widely studied, the behavior of hydrogels with average distances between ionic species larger than the size of surfactant molecule remains less explored.

Adsorption of surfactant molecules within weakly charged hydrogels does not guarantee sufficient proximity to favor aggregation. In the present study, effects of two surfactants in affecting swelling volume of a limited range of weakly charged hydrogels (< 1 mol%) are explored. Surfactant aggregates are destabilized in the presence of macrocycles forming inclusion complexes with the lipophilic regions of amphiphilic molecules [30, 31].

Cyclodextrins (CD's) are a group of well-known macrocyclic carbohydrates, with the primary hydroxyl groups on the narrow (primary) side and the secondary hydroxyl groups on the wider (secondary) side. The resulting hydrophobic cavity and a hydrophilic outside surface [32, 33], support the capability of forming reversible non-covalent host–guest inclusion complexes with hydrophobic molecules such as surfactants [30, 34-36]. As a consequence of the binding process, some properties of the target molecules can be dramatically changed. This is the case of amphiphiles forming micelles or other types of aggregates. Thus, introducing CDs to a solution containing micelles of amphiphilic molecules alter the equilibrium of the self-assembled micellar state thus leading to destabilization of the aggregates [37]. These phenomena attract considerable interests in several fields [31, 38, 39].

The aim of the present work is to monitor changes in hydrogel swelling volume associated with weakly charged hydrogel – surfactant supramolecular self-assembly in a broad range of surfactant concentrations at high precision with respect to volume changes. The hydrogels charge densities were chosen to provide the average distances between charges inside hydrogel network larger than the size of the surfactant molecule. Secondly, we investigate the changes a surfactant equilibrated hydrogel undergo in the presence of cyclodextrins that are reported to form complexes with the surfactants. The presence of cyclodextrins is expected to induce destabilization of the hydrogel-surfactant self-assembled structures. A key feature of the present work is the application of a fiber optic based interferometer to provide *in-situ* high resolution data of the hydrogel swelling. This

monitoring tool is superior to the gravimetric and microscopic techniques commonly used [40, 41] in hydrogel swelling studies. Alongside the interferometric investigation, we apply _ENREF_71 confocal laser scanning microscopy imaging to interrogate the distribution of surfactant microdomains containing the fluorescent probe perylene [42] within the hydrogel. Perylene adsorb preferentially in hydrophobic domains _ENREF_72 such as the interior of surfactant micelles, and exhibit enhanced fluorescence quantum yields in such environment [43]. The identification of the distribution e.g., adsorbed preferentially only at the outermost region of the hydrogel forming shell/stagnant layer similar to that reported by Nilsson and Hansson [44] or more homogenously, will be used for the interpretation of the interferometric data.

2. Experimental Section

2.1. Materials. Acrylamide (AAM, 99%, Sigma), N,N′ -Methylenebisacrylamide (Bis, 99%, Acros organics), 2-acrylamido-2-methyl-1-propanesulfonic acid (AMPSA, 99%, Aldrich), 1-hydroxycyclohexyl phenyl ketone (99%, Aldrich), sodium chloride (NaCl, 99.5%, Fluka), squalane (99%, Aldrich), dimethyl sulfoxide (DMSO, 99.9%, Sigma) were used as received for the preparation of the hydrogels. Cetyltrimethylammonium bromide (CTAB, Tokyo Chemical Industry, TCI), dodecyltrimethylammonium bromide (DTAB, TCI), α-cyclodextrin (α-CD, 98%, Fluka), β-cyclodextrin (β-CD, 97%, SAFC), methyl-β-cyclodextrin (m-β-CD, 97%, Aldrich), γ-cyclodextrin (γ-CD, 99%, Aldrich), and perylene (sublimed grade, ≥ 99.5% Aldrich) were used as received for determination of swelling properties of the hydrogels under various conditions. Deionized water (resistivity 18.2 MΩ×cm, obtained using a Millipore setup) was used for all aqueous solutions.

2.2. Anionic hydrogels. The appropriate amounts of acrylamide and bisacrylamide were dissolved in the deionized water to yield 30 wt% AAM and 3, 6 and 12 mol% Bis relative to AAM. AMPSA was dissolved in water in a separate vial. Photoinitiator was dissolved in DMSO. The three solutions were mixed together yielding 10 wt% of AAM, 0.22, 0.44 and 0.88 mol% AMPSA relative to AAM, 3, 6 or 12 mol% Bis relative to AAM, and 0.15 mol% of initiator relative to AAM in the pregel solutions. Aliquots of the pre-gel solutions were deposited on the tip of the functionalized fiber and polymerized as described [1-4, 45]. Following the polymerization, the hydrogels were washed with deionized water for at least one day to remove possible unpolymerized monomers and other impurities. The resulting hydrogels attached to the end of the optical fiber adapted a nearly hemispherical shape with a radius of about 50 μm.

2.3. Interferometric characterization of hydrogel swelling. All experiments were carried out at room temperature with the hydrogels immersed in the aqueous solution under constant agitation using a magnetic stirrer. The hydrogels covalently linked to the end of the optical fibers were protected against mechanical damage during exposure to changing solvent by locating them within ~~a~~ glass tubes with an inner diameter of about 5 mm. The hydrogels were equilibrated by immersion in 40 ml of deionized water (equilibrium indicated by fluctuations in phase signal of the interferometer less than the resolution limit). Aliquots of concentrated surfactant solutions were pipetted to the constantly stirred immersing aqueous solution. The swelling response of the hydrogels to the stepwise increase of the surfactant concentration were determined by the interferometric technique described in detail elsewhere [1]. The monitoring of changes in hydrogel swelling on exposure to cyclodextrins was carried out by first equilibration of the hydrogels in 40 ml of aqueous surfactant solutions (concentrations

either 10^{-4} M DTAB, 2×10^{-3} M DTAB or 5×10^{-4} M CTAB) followed subsequently by stepwise increase of cyclodextrin concentrations.

The change in the optical length, Δl_{opt}, was extracted from determined phase change of the interferometric wave due to its superior resolution compared to data based on the intensity [1]. Parameter Δl_{opt} was calculated based on the experimentally determined change in phase of the interference wave, $\Delta\varphi$, according to Eq. 1:

$$\Delta l_{opt} = \frac{\Delta\varphi\,\lambda_0}{4\pi} \qquad (1)$$

where λ_0 is the center wavelength of the light source (1550 nm). Optical length changes were followed with 2 nm resolution and sampling rate of 1 Hz. The magnitude of changes in Δl_{opt} that can be determined is limited by the periodicity of the phase (Eq. 1), practically limiting Δl_{opt} to less than $\lambda_0/2$ for consecutive determinations. We employ the changes in the optical length of the hydrogel, Δl_{opt}, relative to the overall optical length of AAM-*co*-AMPSA hydrogels l_{opt}: $S = \Delta l_{opt}/l_{opt}$, as a first parameter for changes of the hydrogel swelling. Parameter Δl_{opt} is determined relative to l_{opt} selected as the reference state for each experimental series. The changes in the degree of swelling associated with subsequent surfactant/cyclodextrin additions were followed as function of time. The ratio $\Delta l_{opt}/l_{opt}$ was empirically observed to change exponentially with time, either equilibration to a new plateau maximum or exponential decay, for hydrogel swelling or deswelling processes, respectively. The swelling kinetics were therefore analyzed based on an apparent first order rate process of S for each step-change in concentration in the immersing bath. Thus, the kinetics of both swelling and deswelling processes were represented by an apparent equilibration time constant ($\tau_{1/2} = \ln 2/k$) by fitting $\Delta l_{opt}(t) \propto e^{-kt}$ to the experimental data for each level of surfactant or cyclodextrin concentration.

2.4. Confocal laser scanning microscopy imaging of AAM-*co*-AMPSA hydrogel with bound CTAB. Confocal laser scanning microscopy imaging experiments used to determine surfactant distribution inside hydrogels were carried out according to the adopted procedure described elsewhere [27]. Perylene was recrystallized from acetone on the walls of flat-bottom flask, and the solvent removed using a water pump. The flask was filled with MQ water and left in ultrasound bath for three hours. The resulting solution was stored in dark (overnight, room temperature) followed by filtering (syringe filter, 0.45 μm pore diameter). CTAB was dissolved in the aqueous perylene solution to a concentration of 0.5 mM. A hydrogel at the end of the optical fiber (0.88 mol% AMPSA, 3mol% Bis) was equilibrated in the CTAB/perylene aq. solution overnight and imaged using confocal microscopy.

The image of a middle section of the hydrogel was taken using confocal laser scanning microscopy (LSM 510 Meta, Carl Zeiss Jena GmbH, Jena, Germany) equipped with an Multiphoton laser and LSM 4.2 software. The image was acquired using 40×magnificaton water immersion objective (C-Apochromat with numerical aperture N.A. = 1.2), and employing two-photon excitation, wavelength λ_{ex} = 750 nm and an emission band pass filter: 387-580 nm in front of PMT detector.

3. Results

3.1. Weakly charged anionic hydrogels immersed in surfactant solutions. The high resolution interferometric technique was employed for monitoring ~~of~~ the AAM-*co*-AMPSA hydrogel swelling when exposed to increasing concentrations of DTAB or CTAB surfactants. Figure 1A shows the equilibrium of the swelling parameter ($\Delta l_{opt}/l_{opt}$) of the hydrogels with increasing surfactant (DTAB or CTAB) concentrations in the immersing aqueous solution. The increase of DTAB concentration from 10^{-7}M caused hydrogels swelling up to DTAB concentrations of 8.5×10^{-5}, 1.6×10^{-4}, 2.1×10^{-4} M for the anionic hydrogels with increasing

charge density (mol fraction of AMPSA of 0.22, 0.44 and 0.88 mol% relative to AAM, respectively). Deswelling was observed for further increase in DTAB concentrations.

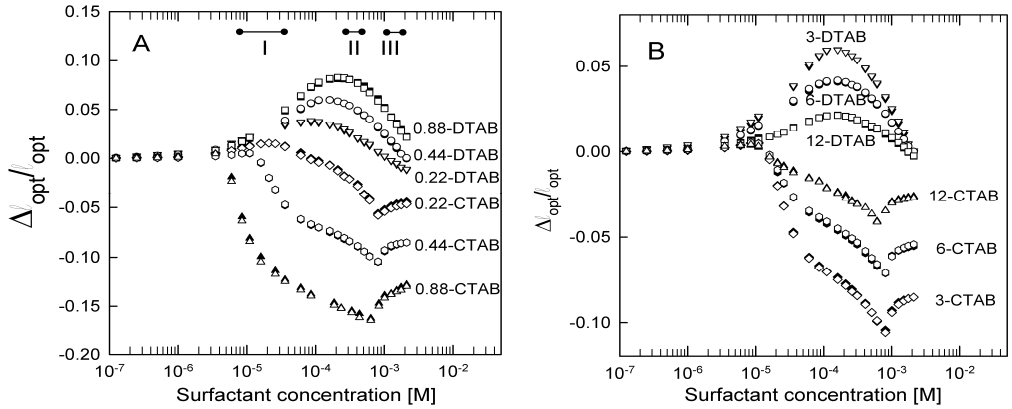

Figure 1. Swelling ratio parameter ($\Delta l_{opt}/l_{opt}$) versus surfactant (DTAB or CTAB) concentration for AAM-*co*-AMPSA hydrogels with A) varied charge densities (0.22, 0.44, and 0.88 mol% AMPSA indicated by the numerical prefix) and constant 3 mol% Bis crosslink density and B) with varied crosslink density (3, 6, 12 mol% Bis indicated by the numerical prefix) at constant charge density 0.44 mol% AMPSA. The measurements were carried out at least two times (open and filled symbols for each experimental series) at room temperature. The regions I, II and III depict surfactant concentration ranges selected for display of time-dependence of Δl_{opt} (Fig. 2).

The anionic hydrogels swelled only slightly at very low CTAB concentrations and significantly deswelled beyond 26, 11, and 3.5×10^{-6} M CTAB for 0.22, 0.44 and 0.88 mol% AMPSA hydrogels, respectively. The hydrogels showed reduced equilibrium swelling up to CTAB concentration of about 0.8 mM almost independent on the charge density of the hydrogel. This CTAB concentration of 0.8 mM coincides with the critical micelle concentration of the surfactant in water determined based on surface tension measurements [46]. The magnitude of hydrogel swelling/deswelling in the presence of surfactants was larger

for increasing anionic character of the hydrogels (Fig. 1A). The surfactant induced changes in the hydrogel swelling at constant charge density of the network were generally reduced with increasing crosslink density (Fig. 1B). The maximum deswelling induced by CTAB was 10.4%, 7.1% and 4.1% for 3, 6 and 12 mol% Bis, respectively (Fig. S1) for the 0.44mol% AMPSA hydrogels.

Figure 2 displays selected data for the kinetics of the change in the optical length of the hydrogel in response to stepwise increase of DTAB surfactant concentration in the three different concentration ranges: I 8.5-36 μM, II 261-411 μM and III 811-1261 μM (indicated in Fig. 1). The hydrogels swells in region I of [DTAB], while shrinking in regions II and III. The experimentally determined time dependences of Δl_{opt} following a step change in [DTAB] (Fig. 2) were used to estimate the kinetic parameter $\tau_{1/2}$ (Fig. 3). Parameter $\tau_{1/2}$ was in the order of 100 s in region I of [DTAB] (Fig. 3). For stepwise increased [DTAB], parameter $\tau_{1/2}$ was almost stable at a plateau of about 100 s followed by an approximately 50 fold reduction to 2-4 s, with a transitions occurring at [DTAB] of 35, 100 and 260 μM for 0.22, 0.44 and 0.88 mol% AMPSA hydrogels, respectively. Increasing the [DTAB] beyond 1 mM yielded an almost [DTAB] independent $\tau_{1/2}$. Note that various regions of [DTAB] represent either hydrogel swelling or deswelling (Fig. 1).

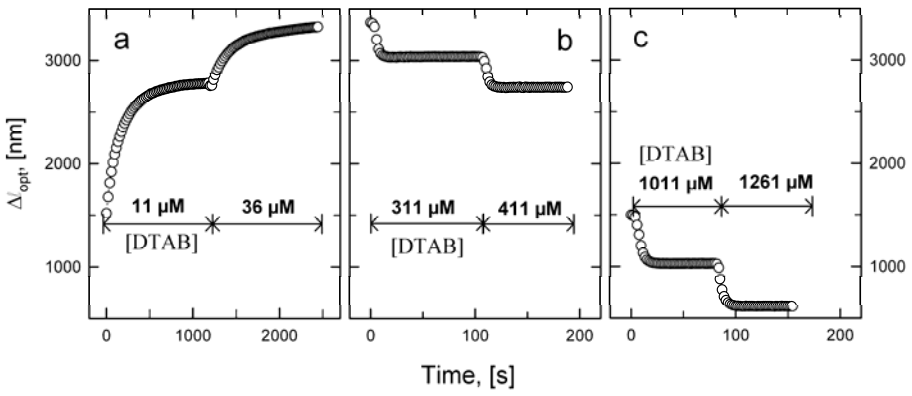

Figure 2. Changes in optical length versus time for 0.44 mol% AMPSA hydrogels crosslinked with 3mol% Bis in response to stepwise increased DTAB concentrations. The data are selected from region I (a), II (b) and III (c) depicted in Fig. 1a.

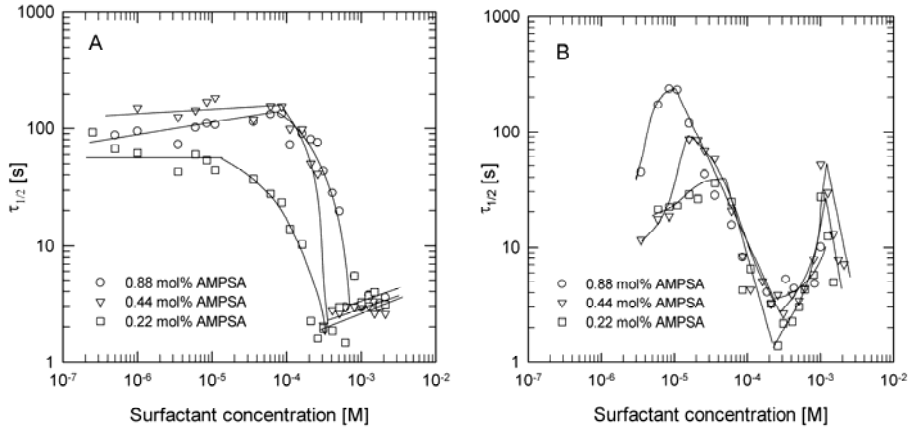

Figure 3. Equilibration half-life time of changes in optical length associated with anionic hydrogels swelling versus surfactant concentration for DTAB (A) and CTAB (B). The data were obtained from changes in optical length versus time for stepwise increase in surfactant concentrations as exemplified in Fig. 2 for DTAB, and employing anionic hydrogels with 0.22, 0.44 and 0.88 mol% AMPSA and 3mol% Bis crosslink density. The surfactant concentrations denoted are [DTAB] or [CTAB] after their stepwise increase.

The kinetics of the hydrogel swelling induced by stepwise changes in CTAB display similar trends as for DTAB, but more accentuated (Fig. 3). At low [CTAB] $\tau_{1/2}$ increases with increasing surfactant concentration up to 60, 16 and 8.5 μM for 0.22, 0.44 and 0.88 mol% AMPSA hydrogels reaching the values of 35, 87 and 240 s, respectively. Further increase of [CTAB] above these maxima of $\tau_{1/2}$ yields reduction of $\tau_{1/2.}$ Parameter $\tau_{1/2}$ reaches the minimum value of few seconds at CTAB concentration of about 0.2 mM, independent of anionic charge density of the hydrogels. In the [CTAB] range from 0.2 to 0.8 mM in the immersing solution, $\tau_{1/2}$ shows an increase and reaches a maximum at the CTAB

concentration of 0.8 mM slightly lower than cmc of that surfactant 0.98 mM [47]. This is followed by a decline in $\tau_{1/2}$ for increased [CTAB] above cmc.

Laser confocal imaging of a AAM-*co*-AMPSA hydrogel equilibrated in perylene saturated 0.5 mM CTAB was employed to obtain information on the distribution of surfactants within the hydrogel. The optical micrograph (Fig. 4) indicates a homogeneous distribution of the perylene fluorescence intensity within the hemispherical hydrogel attached to the optical fiber. This observation suggests a homogeneous distribution of surfactant micelles inside the weakly charged hydrogel studied here. This is in contrast with the shell like surfactant association on hydrogels reported for highly charged hydrogels [44].

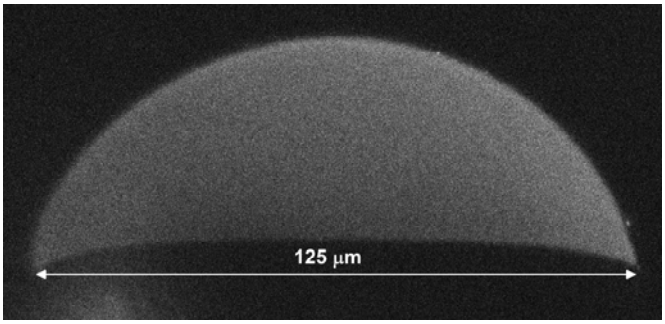

Figure 4. Confocal laser scanning optical micrograph of AAM-*co*-AMPSA (0.88 mol% AMPSA, 3 mol% Bis) hydrogel, at the end of an optical fiber, equilibrated in perylene-0.5mM CTAB aqueous solution. The fluorescent perylene preferentially embedded in the CTAB micelles indicate the distribution of CTAB surfactant micelles within the hydrogel. The hydrogel appearing with a hemispherical shape is covalently linked to optical fiber (diameter 125 μm).

3.2. Anionic hydrogels equilibrated with surfactant immersed in cyclodextrin solutions. Cyclodextrins known to form inclusion complexes with surfactants [30, 31, 48-51] were expected to destabilize the pre-formed hydrogel-surfactant complexes. The influence of

different types of cyclodextrins α-CD, β-CD, m-β-CD and γ-CD on hydrogel swelling ratio ($\Delta l_{opt}/l_{opt}$) was studied. For that purpose anionic hydrogels consisting of 0.44 mol% AMPSA, 3 mol% Bis were pre-equilibrated in 10^{-4} M and 2×10^{-3} M DTAB and 5×10^{-4} M CTAB aqueous solution followed by exposure to subsequent step-wise increase in cyclodextrin concentration from 10^{-6} to 5×10^{-3} M. (Figs. 5 and 6).

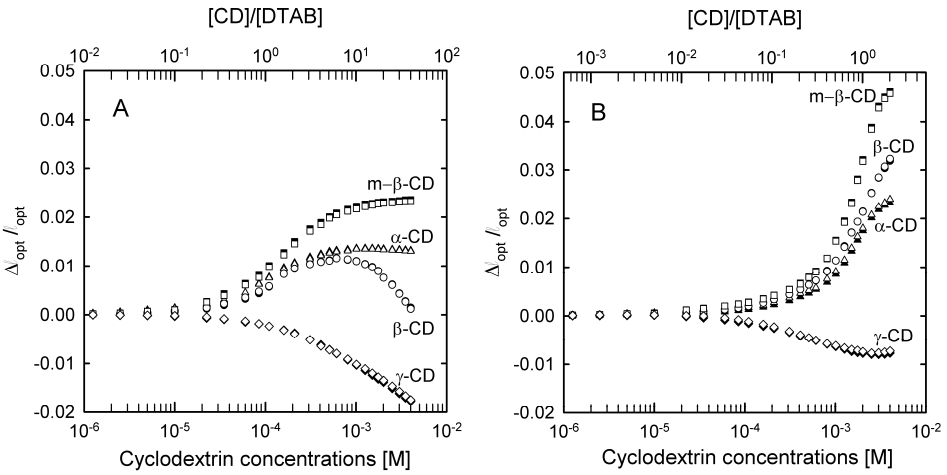

Figure 5. Swelling ratio parameter ($\Delta l_{opt}/l_{opt}$) versus cyclodextrin concentration of anionic hydrogels (0.44 mol% AMPSA, 3 mol% Bis) pre-equilibrated in A) 10^{-4} M and B) 2×10^{-3} M DTAB. The measurements were carried out at least two times at room temperature. The upper scale shows the ratio between the cyclodextrin concentrations and the pre-equilibration surfactant concentration.

The pre-equilibrated hydrogels in DTAB swelled for α-CD, β-CD and m-β-CD concentrations above 10^{-5} M. The changes in the swelling ratio were larger for the hydrogel pre-equilibrated at higher surfactant concentration (Fig. 5). Cyclodextrin m-β-CD induced the largest hydrogel swelling compared to α- and β-CD. In contrast, γ-CD induced a continuous decrease of swelling ratio. The aqueous solutions with the four cyclodextrins all induced swelling of the hydrogels equilibrated in CTAB (Fig 6). The changes in swelling ratio associated with

cyclodextrins added to the immersing solution were substantially larger for the hydrogels pre-equilibrated with CTAB than with DTAB. The magnitude of the swelling for the CTAB pre-equilibrated hydrogels were largest for the m-β-CD, followed by β-CD and α-CD, while γ-CD induced a significantly less swelling response.

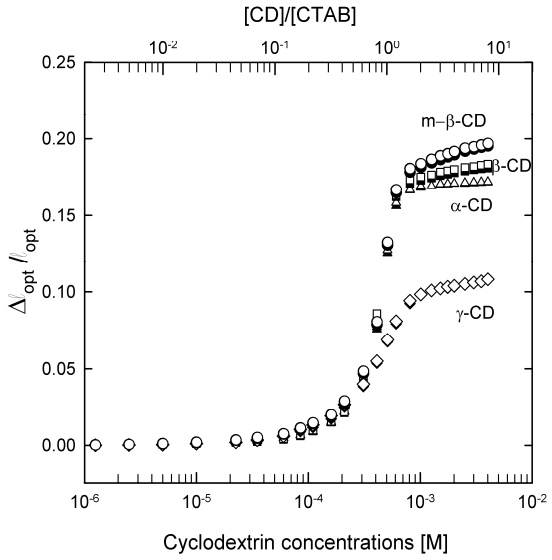

Figure 6. Swelling ratio parameter ($\Delta l_{opt}/l_{opt}$) versus cyclodextrin concentration for anionic hydrogels (0.44 mol% AMPSA, 3 mol% Bis) pre-equilibrated in 5×10^{-4} M CTAB. The measurements were carried out at least two times at room temperature. The upper scale shows the ratio between the cyclodextrin concentrations and the pre-equilibration surfactant concentration.

The readjustments to a new equilibrium state associated with the increase of the concentrations of cyclodextrins were quick (Fig. 7) and the equilibration half-lifetimes were no longer than few seconds. This range of $\tau_{1/2}$ was found throughout the explored CD concentration range. The equilibration was much faster comparing to the kinetics of swelling associated with surfactant binding inside the hydrogels.

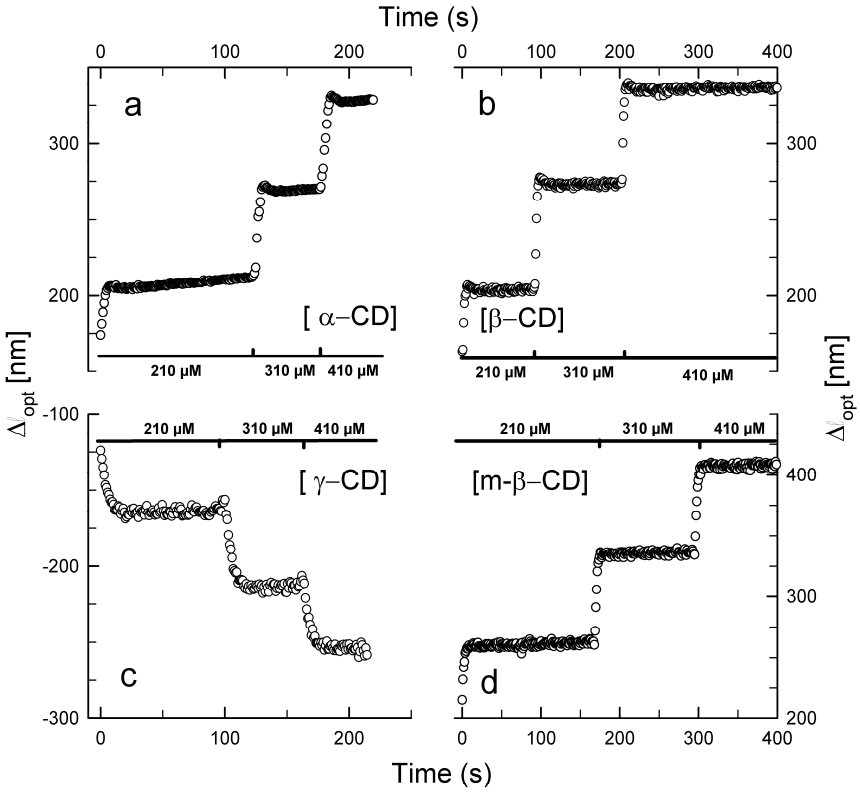

Figure 7. Changes in optical length of anionic hydrogels (0.44 mol% AMPSA, 3 mol% Bis) pre-equilibrated in 2×10^{-3} M of DTAB solution in response to stepwise increase in concentration of a) α-, b) β-, c) γ- and d) m-β-cyclodextrins. The concentrations of the cyclodextrins from 210 to 410 μM are indicated.

4. Discussion

The net change of the optical length within the hydrogels used as primary experimental parameters following exposure to surfactant solutions and also subsequent addition of cyclodextrins can be affected by changes in optical properties within the light path and/or changes in physical length of the optical pathway. The net change in Δl_{opt} through the hydrogel can be expressed as the difference of the integrals of the refractive indices along the optical path for the two conditions being compared:

$$\Delta l_{opt} = \int_0^{l_2} n_2(l)dl - \int_0^{l_1} n_1(l)dl \qquad (2)$$

where l_i, n_i (i=1,2) are the total physical lengths of the optical path and refractive index at the conditions indicated by the index, respectively. The recorded signal thus only provides information related to differences of the integral of the refractive indices along the optical path for the conditions being compared rather than changes in distribution of *n* in the two states. The changes in the optical length combined with information on the refractive index as derived from Eq. 2 is reported to correspond to changes in physical dimension as determined by confocal microscopy [52]. The result of a homogeneous distribution of the surfactant obtained by confocal imaging in the present case (Fig. 4) suggests that it is not necessary to consider distribution of the surfactant and its possible influence of the refractive indices in these cases. Due to the concentration ranges used, we argue that the changes in physical length of the hydrogels are the dominating contribution to the observed changes in Δl_{opt}.

Introducing the mean refractive indices along the optical path in the two states:

$$\langle n_i \rangle = l_i^{-1} \int_0^{l_i} n_i(l)dl \ , \ \mathrm{i} = 1,2 \qquad (3)$$

in Eq. 2 yields:

$$\Delta l_{opt} = \langle n_2 \rangle l_2 - \langle n_1 \rangle l_1 \approx \langle n_1 \rangle \Delta l + l_1 \Delta n \qquad (4)$$

where Δl and Δn are the differences in length of the optical path and mean refractive indices, respectively. An estimate of the relative importance of the two terms identified in Eq. 4, for the exposure of the anionic hydrogels to the surfactants and cyclodextrins can be made based on the optical properties of the materials within the applied concentration range. The molar concentration of charges for the 0.88 mol% AMPSA hydrogel in the relaxed state was calculated to be 12.3 mM. Assuming a charged balanced association of surfactant molecules without any dimensional change of hydrogel correspond to a surfactant concentration equal to

3.25 g/l. The refractive index increments for DTAB in NaBr salt aqueous solution and for cyclodextrins in aqueous solution were found to be 0.149 ml/g [53] and 0.148 ml/g [54], respectively. Charged balanced DTAB association in the 0.88 mol% AMPSA hydrogel is thus estimated to change the hydrogel refractive index by $\Delta n = 0.00048$. The data obtained on the distribution of the surfactant (Fig. 4) also indicate that the assumption of homogeneous loading of surfactant within the hydrogel is valid. Thus, the contribution to $\Delta l_{opt}/l_{opt}$ from change in Δn at constant physical length is estimated to $\Delta l_{opt}/l_{opt} = \Delta n/n = 0.00035$ using refractive index 1.361 [1] for acrylamide based hydrogels. This contrasts most of the observed relative changes $\Delta l_{opt}/l_{opt}$, typically 100 times or larger. In the following, we therefore attribute the observed changes $\Delta l_{opt}/l_{opt}$ only to changes in the physical length of the hydrogel materials immersed in the aqueous solutions.

Equilibration of the anionic hydrogels in surfactant and subsequently in cyclodextrin aqueous solutions is therefore interpreted in view of cationic surfactants binding to the network, surfactant aggregation mediated hydrogel deswelling, cyclodextrin interaction with the surfactants and concomitant effect on swelling equilibrium. A schematic illustration of hydrogel collapse in the presence of aggregating surfactants and hydrogel swelling due to destabilization of surfactant complexes by cyclodextrin is presented in Fig. 8.

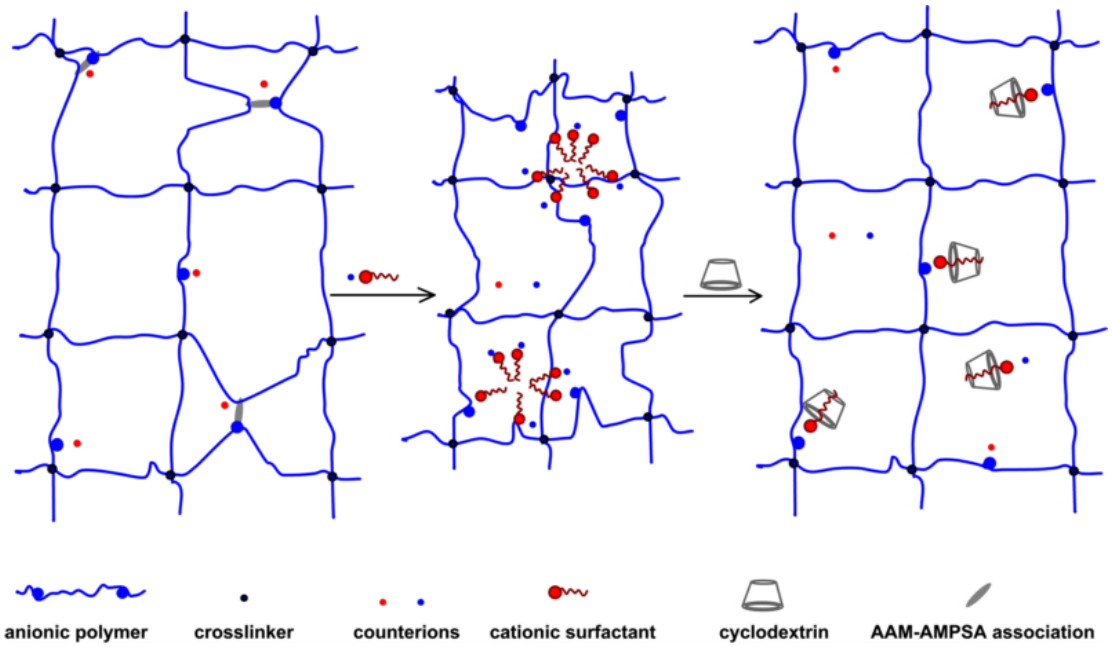

Figure 8. Schematic illustration of surfactant aggregation induced hydrogel collapse and re-swelling in the presence of cyclodextrins forming inclusion complexes with surfactant molecules. Screening effect of AAM-AMPSA associations is also illustrated.

Changes in hydrogel swelling resulting from increase of the number of charges inside a hydrogel network or change in the crosslink density, as accounted for within the Flory-Rehner-Donnan theory, are applied as a qualitative framework in the following. The lack of a surfactant enriched shell observed in the present weakly charged hydrogels (Fig. 4) is in contrast with surfactants assembled as a layer at the outermost part of more highly charged hydrogels yielding a balloon type of swelling behavior [44]. Thus, the theoretical framework can be applied assuming a homogeneous material. The observed AAM-*co*-AMPSA hydrogel swelling at low surfactant concentration (DTAB, Fig. 1) can be accounted for in view of the intrinsic nature of these hydrogels. All the AAM-*co*-AMPSA hydrogels were crosslinked with stable covalent crosslinker Bis, but in addition association between strongly charged sulfonic acid group and weakly charged amide group is likely [55, 56]. Those interactions may lead to the formation of weak physical crosslinks [57]. These interactions may be

screened with concomitant effect of destabilizing the crosslinks in the presence of low molecular weight salt (Fig. S2) or in our case surfactant molecules. Such a reduction of the number of crosslinks may result in hydrogel swelling. The swelling at low surfactant concentrations was much less pronounced in the case of CTAB – surfactant with longer aliphatic chain than DTAB (Fig 1). The hydrogels only slightly swelled at the CTAB concentrations lower than 10^{-5} M and significantly deswelled for increasing [CTAB] larger than 10^{-5} M. The pronounced hydrogel deswelling is suggested to arise from self-assembling of the adsorbed surfactant molecules inside the hydrogel network. Due to this aggregation the concentration of mobile counterions inside the gel decreases thus reducing the internal osmotic pressure of the gel [58]. Surfactant micelles interconnecting different elastically active chains may additionally contribute to hydrogel deswelling by increasing the crosslinking density [58]. The finding that these surfactant dependent hydrogel swelling are larger for the more anionic hydrogels and less for the more highly crosslinked hydrogels (Fig. 1) are in line with the suggested molecular model. Increasing the anionic polymer network charge density increases the electrostatic driven surfactant association and concomitant micelle formation. Increasing the covalent crosslink density strengthens the relative importance of the elastic restoring contribution to the free energy of ionic hydrogel swelling. Figure 9 depict estimated data for CTAB deswelling in the hypothetical case of non-existing physical crosslinks from charged sulfonic acid group and weakly charged amide group that concomitantly are screened by the surfactant. This indicate that the “bumps” in the CTAB concentration dependent deswelling, e.g., in the range 10^{-4} to 10^{-5} M of CTAB (Figs. 9 and 1), are due to net effects of surfactant association with concomitant micelle formation of CTAB and the destabilization of physical crosslinks by screening of the sulfonic acid - amide group interactions.

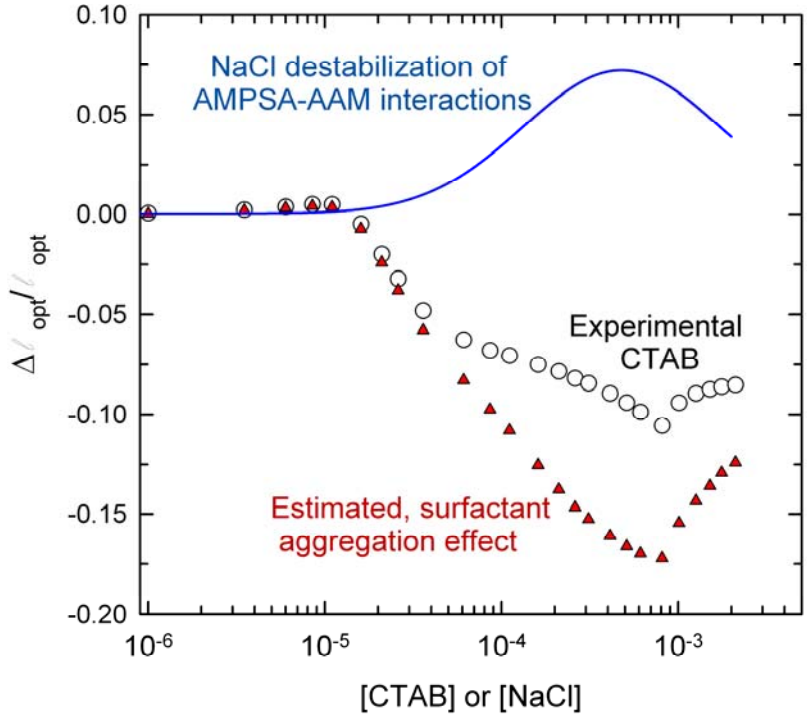

Figure 9. Illustration of the relative importance of micelle formation and screening of ionic sulfonic acid - amide group estimated in the case of CTAB. Swelling ratio parameter ($\Delta l_{opt}/l_{opt}$) versus surfactant CTAB concentration for AAM-*co*-AMPSA hydrogels (0.44mol% AMPSA, 3 mol% Bis, Fig. 1) (open circles), fit of the swelling ratio versus the ionic strength determined versus NaCl concentration (Fig. S2) (blue line) and the hypothetical case of no ionic crosslinks in the hydrogel calculated by the difference in these data (red triangles).

The hydrogels deswell until the concentration of CTAB in the immersing solution reaches 0.8 mM. The deswelling of the hydrogels is most pronounced at this surfactant concentration. Increasing [CTAB] beyond this value causes gradual increase of the hydrogel optical length relative to that at 0.8 mM. The hydrogel reswelling beyond this concentration is likely due to adsorption of excessive charged surfactant molecules [59] and is dominated

by increasing osmotic pressure. Such excessive adsorption of surfactant is suggested to be accounted for by second cooperative binding process at concentration preceding cmc of the surfactant, also referred to as second critical aggregation concentration, cac2 [47]. For the shorter DTAB the effect of collective aggregation occurs at higher surfactant concentrations than for CTAB.

Exposure of the surfactant equilibrated hydrogels to cyclodextrins resulted in increasing the optical length within the hydrogel. Among the three mechanisms accounted for by the Flory-Rehner theory, it appears that effects of γ-cyclodextrin through changes in crosslink density are more likely than alterations of miscibility or osmotic pressure effects. However, due to rather small changes seen ~~in~~ particular in the case of DTAB induced swelling, effects through the other mechanisms cannot be ruled out. With this in mind, the swelling is suggested to be ascribed to the formation of surfactant-cyclodextrin inclusion complexes leading to destabilization of the surfactant complexes. The hydrogel-DTAB complex systems behaved differently at presence of γ-CD compared to the other types of cyclic carbohydrates. In this case the hydrogel deswelling was observed. γ-CD in contrast to α-CD, β-CD and methyl-β-CD, may host two guest surfactant molecules [60, 61]. The formation of double stranded complexes of polyethylene-glycol and γ-CD was shown to lead to the gelation [62, 63]. The same effect may occur in hydrogel-DTAB system where γ-CD may play a role as a supramolecular crosslinker by hosting two DTAB molecules leading to the hydrogel shrinkage. γ-CD may supply additional binding sites for the surfactant molecules present inside the hydrogel network that are not yet involved in micellar crosslinks. This additional crosslinking should be more dominant the less surfactant bound to the hydrogel network is involved in micelles. This is in line with the experimental observation of a more pronounced γ-CD induced deswelling at lower DTAB concentration (10^{-4} M, aggregation onset), than at the higher concentration ($2 \cdot 10^{-3}$ M) where a larger

fraction of the bound surfactant molecules is involved in micellar, physical crosslinks (Figs. 5a and b). The same phenomenon may explain why the swelling of CTAB-hydrogel system in the presence of γ-CD is less pronounced than in the case of α-CD, β-CD and methyl-β-CD. In case of CTAB surfactant, at the concentration of $5 \cdot 10^{-4}$ M micelles are already formed leading to significant deswelling. Overall, the results suggest that there are two competing processes in hydrogel-surfactant-γ-CD system, one is the destabilization of surfactant micellar aggregates leading to swelling and another is the formation of surfactant-γ-CD-surfactant bridges that may lead to collapse. Therefore, observed swelling/deswelling changes are net changes resulting from the two concomitant phenomena.

The apparent critical collapse concentrations (ccc) for the hydrogels were estimated based on swelling/deswelling curves vs. surfactant concentration (Table 1).

Table 1. Critical concentrations and free Gibbs energy of CTAB aggregation for 3 mol% BIS hydrogel-surfactant systems.

		AMPSA content, mol %		
Property	Surfactant	0.22	0.44	0.88
ccc, μM	DTAB	86	161	211
	CTAB	26	11	4
ΔG^0_a, kJ/mol	CTAB	-26.0	-28.1	-30.9

As the ccc nearly coincide with surfactant critical aggregation concentration (cac) [25] the Gibbs free energy of aggregation (Table 1) was calculated based on Eq. 5 [64]:

$$\Delta G^0_a = RT\ln(cac) \quad (5)$$

The free energy of CTAB surfactant aggregation inside the hydrogels was found to be increasingly negative with increasing charge density of the hydrogel. Thus, the increase of AMPSA molar content resulted in higher aggregation driving forces. The apparent ccc is observed to increase with increasing AMPSA fraction in the hydrogel in the case of DTAB. This is different from the trend commonly observed for highly charged hydrogels and polymers interacting with oppositely charged surfactants [28, 65]. It is suggested that the present observation (Fig. 1) is due to the relative importance of two processes: 1) destabilization of sulfonic acid – amide group interactions leading to hydrogel swelling and 2) formation of additional physical crosslinks resulting from surfactant molecules aggregation inside hydrogel network. Depending on which of the two processes dominates the hydrogel swells or deswells. The DTAB concentration for which the collapse starts should rather be attributed to the beginning of domination of the surfactant aggregation process over disruption of sulfonic acid – amide group interactions than the beginning of surfactant aggregation. In other words: the onset of micelle formation may precede hydrogel collapse thus swelling of the hydrogel-DTAB upon cyclodextrins exposure may be observed for [DTAB] lower than critical collapse concentration. In the case of CTAB high charge density causes stronger association of surfactant molecules inside a hydrogel and therefore the concentration of CTAB inside a hydrogel necessary for aggregation and a concomitant hydrogel deswelling is attained at lower [CTAB] in the external solution. Therefore only slight hydrogels swelling is observed at the CTAB concentrations preceding significant collapse. DTAB with shorter hydrophobic tail is not able to aggregate at such a low concentrations as CTAB. Instead, the molecules act as low molecular salt to screen interactions between sulfonic acid and amide groups and concomitant hydrogel swelling (Fig. 1). The swelling is ~~the~~ more pronounced the higher the charge density of the hydrogel. The

hydrogel swelling associated with the screening of the sulfonic acid – amide group interactions can accentuate the need to increase the surfactant concentration to initiate micelle formation due to concomitant reduced network charge density (per unit volume) associated with the swelling.

The kinetics of hydrogel swelling/deswelling response on incremental changes to surfactants or cyclodextrins can be compared to various possible rate limiting factors in the process. It is previously reported that ionic hydrogels of similar size display time constants of about 2-3 seconds for changes in ionic strength and 95-130 seconds for changes in pH [1]. Additionally, kinetics constants of 100 seconds and larger for swelling of phenylboronic acid incorporated hydrogels associated with changes in glucose have been reported [3]. These data indicated that the swelling kinetics associated with changes in ionic strength reflected the limit due to the diffusion of the network chains, while the others were limited by the rate of interactions among the involved species. Thus, also for time constants larger than 2-3 seconds observed in the present data (Fig. 3), it is assumed that the kinetics of hydrogel swelling in the presence of surfactants reflect kinetics of molecules self-assembly inside the hydrogel material. The kinetics of hydrogel swelling induced by the presence of diluted surfactants were much slower compared to the processes inducing deswelling (Fig. 3). This may be explained by considering the processes which drive the swelling or collapse. The swelling occurs due to slow association and assembling of surfactant molecules concomitant with ion exchange and physical crosslink breakage while deswelling results from cooperative process of surfactant micelle formation [66]. The differences in nature of the two processes driving either hydrogel swelling or deswelling may explain the differences in the kinetics of hydrogel response. In contrast to the rather slow, and concentration dependent surfactant induced hydrogel swelling readjustment, the kinetic constants associated with the

cyclodextrin exposure are comparatively small, and approach that for the network readjustment of 2-3 seconds.

5. Conclusions

A high resolution interferometric technique has been successfully applied to study changes in equilibrium swelling ratio and swelling/deswelling kinetics associated with supramolecular complex formation in hydrogel - amphiphilic molecule – macrocycle three-component system. The technique supports in-situ determination of the hydrogel optical length changes associated with anionic hydrogel- cationic surfactant complexation processes and the changes associated with destabilization of the formed hydrogel-surfactant complexes with different types of cyclodextrins (α-CD, β-CD, methyl-β-CD and γ-CD). The high resolution of the technique allowed for monitoring of unexpected swelling of low charge density hydrogels exposed to diluted surfactants which precedes their collapse at higher concentrations of amphiphiles. The results show different type of behaviors for the two surfactants at low concentrations, arising from the differences in the length of surfactant hydrophobic tails. The critical collapse concentration of the hydrogel induced by CTAB decreases with increasing charge density, thus supporting current literature data [28, 65]. At variance, for DTAB there is an apparent increase in the surfactant concentration for the onset of hydrogel deswelling with the increasing charge density of the hydrogel. This is suggested to be accounted for in terms of screening of sulfonic acid – amide group interactions. The importance of two different mechanisms contributing to the AAM-*co*-AMPSA hydrogel response to surfactants: 1) destabilization of sulfonic acid – amide group interactions and 2) formation of additional physical crosslinks resulting from surfactant molecule aggregation inside hydrogel network has been scrutinized. The net effect of these phenomena in the case of DTAB makes it difficult to identify onset of hydrogel collapse with cac, while this is not

the case for CTAB. The kinetics of supramolecular self-assembly inside the hydrogels materials were shown to be a limiting factor for hydrogel swelling rate. The hydrogel-surfactant complexes were destabilized in the presence of cyclodextrins interacting with surfactant hydrophobic tails however γ-cyclodextrin was shown to be less efficient destabilizing agent compared to other cyclodextrins due to its ability to host two surfactant molecules[60, 61] and thus form supramolecular crosslinks.

Acknowledgment

This work was supported by the Norwegian Research Council, contract number 191818/V30. We gratefully acknowledge the skillful technical assistance by senior engineer Astrid Bjørkøy in assisting confocal image acquisition.

References

[1] S. Tierney, D.R. Hjelme, B.T. Stokke, Anal. Chem. 80 (2008) 5086.

[2] S. Tierney, S. Volden, B.T. Stokke, Biosens. Bioelectron. 24 (2009) 2034.

[3] S. Tierney, B.M.H. Falch, D.R. Hjelme, B.T. Stokke, Anal. Chem. 81 (2009) 3630.

[4] S. Tierney, B.T. Stokke, Biomacromolecules 10 (2009) 1619.

[5] M. Gao, K. Gawel, B.T. Stokke, Soft Matter 7 (2011) 1741.

[6] K. Gawel, B.T. Stokke, Soft Matter 7 (2011) 4615.

[7] R. Mansson, H. Bysell, P. Hansson, A. Schmidtchen, M. Malmsten, Biomacromolecules 12 (2011) 419.

[8] M. Malmsten, H. Bysell, P. Hansson, Curr. Opin. Colloid Interface Sci. 15 (2010) 435.

[9] D. Mirejovsky, A.S. Patel, D.D. Rodriguez, T.J. Hunt, Optom. Vis. Sci. 68 (1991) 858.

[10] S. Buck, P.S. Pennefather, H.Y. Xue, J. Grant, Y.L. Cheng, C.J. Allen, Biomacromolecules 5 (2004) 2230.

[11] J.P. Gong, Y. Osada, J. Phys. Chem. 99 (1995) 10971.

[12] P. Hansson, Langmuir 14 (1998) 4059.

[13] H. Okuzaki, Y. Osada, Macromolecules 28 (1995) 4554.

[14] O.E. Philippova, S.G. Starodoubtzev, J. Polym. Sci., Part B: Polym. Phys. 31 (1993) 1471.

[15] P. Hansson, S. Schneider, B. Lindman, J. Phys. Chem. B 106 (2002) 9777.

[16] S. Salmaso, A. Sernenzato, S. Bersani, P. Matricardi, F. Rossi, P. Caliceti, Int. J. Pharm. 345 (2007) 42.

[17] K. Na, K.H. Park, S.W. Kim, Y.H. Bae, J. Controlled Release 69 (2000) 225.

[18] K. Tomoda, K. Makino, Colloid Surf. B-Biointerfaces 55 (2007) 115.

[19] S. Chatterjee, D.S. Lee, M.W. Lee, S.H. Woo, Bioresour. Technol. 101 (2010) 4315.

[20] L.M. Bronstein, O.A. Platonova, A.N. Yakunin, I.M. Yanovskaya, P.M. Valetsky, A.T. Dembo, E.E. Makhaeva, A.V. Mironov, A.R. Khokhlov, Langmuir 14 (1998) 252.

[21] H. Kasgoz, S. Ozgumus, M. Orbay, Polymer 44 (2003) 1785.

[22] Y. Wu, T. Tang, B. Bai, X. Tang, J. Wang, Y. Liu, Polymer 52 (2011) 452.

[23] H. Li, P. Zhang, L. Zhang, T. Zhou, D. Hu, J. Mater. Chem. 19 (2009) 4575.

[24] B. Doumèche, M. Heinemann, J. Büchs, W. Hartmeier, M.B. Ansorge-Schumacher, J. Mol. Catal. B: Enzym. 18 (2002) 19.

[25] P. Hansson, J. Phys. Chem. B 113 (2009) 12903.

[26] E. Hoff, B. Nystrom, B. Lindman, Langmuir 17 (2001) 28.

[27] K. Szczubialka, K. Rosol, M. Nowakowska, J. Appl. Polym. Sci. 102 (2006) 2401.

[28] K. Rosol, K. Szczubialka, B. Jachimska, S. Zapotoczny, M. Nowakowska, J. Appl. Polym. Sci. 107 (2008) 3184.

[29] D. Costa, M.G. Miguel, B. Lindman, J. Phys. Chem. B 111 (2007) 8444.

[30] U.R. Dharmawardana, S.D. Christian, E.E. Tucker, R.W. Taylor, J.F. Scamehorn, Langmuir 9 (1993) 2258.

[31] E. Junquera, G. Tardajos, E. Aicart, Langmuir 9 (1993) 1213.

[32] A. Harada, J. Li, M. Kamachi, Nature 356 (1992) 325.

[33] M.V. Rekharsky, Y. Inoue, Chem. Rev. 98 (1998) 1875.

[34] G.M. Nicolle, A.E. Merbach, Chem. Commun. (2004) 854.

[35] M. Nilsson, C. Cabaleiro-Lago, A.J.M. Valente, O. Söderman, Langmuir 22 (2006) 8663.

[36] L. Jiang, Y. Yan, J. Huang, C. Yu, C. Jin, M. Deng, Y. Wang, J. Phys. Chem. B 114 (2010) 2165.

[37] G. González-Gaitano, A. Compostizo, L. Sánchez-Martín, G. Tardajos, Langmuir 13 (1997) 2235.

[38] D.J. Jobe, R.E. Verrall, E. Junquera, E. Aicart, J. Phys. Chem. 98 (1994) 10814.

[39] H. Mwakibete, D.M. Bloor, E. Wyn-Jones, Langmuir 10 (1994) 3328.

[40] M.J. Molina, M.R. Gomez-Anton, I.F. Pierola, J. Phys. Chem. B 111 (2007) 12066.

[41] X.Z. Zhang, D.Q. Wu, C.C. Chu, Biomaterials 25 (2004) 4719.

[42] M. Nowakowska, J. Storsberg, S. Zapotoczny, J.E. Guillet, New J. Chem. 23 (1999) 617.

[43] J. Olmsted, The Journal of Physical Chemistry 83 (1979) 2581.

[44] P. Nilsson, P. Hansson, J. Colloid Interface Sci. 325 (2008) 316.

[45] S. Tierney, M. Sletmoen, G. Skjak-Braek, B.T. Stokke, Carbohydr. Polym. 80 (2010) 828.

[46] M.A. Bahri, M. Hoebeke, A. Grammenos, L. Delanaye, N. Vandewalle, A. Seret, Colloids Surf., A: Physicochem. Eng. 290 (2006) 206.

[47] B. Naskar, A. Dan, S. Ghosh, V.K. Aswal, S.P. Moulik, J. Mol. Liq. 170 (2012) 1.

[48] W. Eli, W. Chen, Q. Xue, J. Inclusion Phenom. Mol. Recognit. Chem. 38 (2000) 37.

[49] N. Funasaki, H. Yodo, S. Hada, S. Neya, Bull. Chem. Soc. Jpn. 65 (1992) 1323.

[50] T. Loftsson, M. Masson, M.E. Brewster, J. Pharm. Sci. 93 (2004) 1091.

[51] H. Mwakibete, R. Cristantino, D.M. Bloor, E. Wynjones, J.F. Holzwarth, Langmuir 11 (1995) 57.

[52] K. Gawel, M. Gao, B.T. Stokke, European Polymer Journal (2012) http://dx.doi.org/10.1016/j.eurpolymj.2012.07.006

[53] M. Pisárcik, F. Devínsky, E. Svajdlenka, Colloids Surf., A: Physicochem. Eng. 119 (1996) 115.

[54] G.M. Pavlov, E.V. Korneeva, N.A. Smolina, U.S. Schubert, Eur. Biophys. J. Biophys. Lett. 39 (2010) 371.

[55] T. Tominaga, V.R. Tirumala, E.K. Lin, J.P. Gong, H. Furukawa, Y. Osada, W.-l. Wu, Polymer 48 (2007) 7449.

[56] C. Zhang, A.J. Easteal, J. Appl. Polym. Sci. 89 (2003) 1322.

[57] F. Ilmain, T. Tanaka, E. Kokufuta, Nature 349 (1991) 400.

[58] A.R. Khokhlov, E.Y. Kramarenko, E.E. Makhaeva, S.G. Starodubtzev, Macromol. Theory Simul. 1 (1992) 105.

[59] I. Lynch, J. Sjostrom, L. Piculell, J. Phys. Chem. B 109 (2005) 4258.

[60] N. Funasaki, M. Ohigashi, S. Hada, S. Neya, Langmuir 16 (1999) 383.

[61] R. De Lisi, G. Lazzara, S. Milioto, N. Muratore, J. Phys. Chem. B 107 (2003) 13150.

[62] M.-M. Fan, Z.-J. Yu, H.-Y. Luo, S. Zhang, B.-j. Li, Macromol. Rapid Commun. 30 (2009) 897.

[63] A. Harada, J. Li, M. Kamachi, Nature 370 (1994) 126.

[64] K. Kogej, J. Skerjanc, Langmuir 15 (1999) 4251.

[65] J. Travas-Sejdic, A.J. Easteal, Polymer 41 (2000) 7451.

[66] H. Wennerstrom, B. Lindman, Phys. Rep.-Rev. Sec. Phys. Lett. 52 (1979) 1.